*American Journal of Applied Mathematics*
2025, Vol. 13, No. 2, pp. 143-152
https://doi.org/10.11648/j.ajam.20251302.14

Research Article

# Natural Convective Flow and Heat Transfer in a U-Shaped Device with a Solid Strip Using $Al_2O_3$-Water Nanofluid

**Main Uddin Ahammad*, Shohag Hossain Reyad**

Department of Mathematics, Dhaka University of Engineering and Technology, Gazipur, Bangladesh

## Abstract

This research explores the numerical investigation of natural convective heat transfer in a U-shaped device having an internal thermally isolated solid strip through the use of nanofluid. Such configuration along with specified boundary conditions is very demanding for obtaining most favourable cooling efficiency. The nanoparticle alumina ($Al_2O_3$) is considered here to form single-phase nanofluid mixing with pure water corresponds to $Pr$ = 7.0. Galerkin weighted residual based finite element method along with sophisticated software has been adopted for solving the non-dimensional partial differential equations (continuity of mass, momentum and energy) that govern the present problem. The effects of natural convection parameter Rayleigh number varied as $10^4 \le \text{Ra} \le 10^7$ and geometric parameter volume fraction of nanoparticle in the range $0.01 \le \varphi \le 0.1$ on the flow and thermal field as well as heat transfer rate have been analyzed and expressed by streamlines, isotherms and average Nusselt number. Moreover, for better understanding of flow visualization and temperature behaviour velocity profile, temperature profile and temperature gradient magnitude profile are also exposed. Major outcomes of the current work are displayed in both of the tabular and graphical form. The results indicate that the average Nusselt number which is the representative of heat transfer performance rises as both of Rayleigh number and the nanoparticle volume fraction increases which establish the significance of pertinent parameters in respective field.

## Keywords

Natural Convective, Flow, Heat Transfer, U-shaped Device, $Al_2O_3$-Water, Nanofluid

## 1. Introduction

Natural convection in nanofluids has drawn a lot of attention in applications involving heat transfer and thermal management, particularly in confined geometries like U-shaped cavities. Because of their better thermal characteristics over traditional fluids, nanofluid colloid suspensions of nanoparticles in base fluids are excellent choices for enhancing heat transfer rates in a variety of engineering systems. Numerous investigations into the behavior of nanofluids under various enclosure layouts and thermal conditions have been spurred by their enhanced thermal conductivity and distinctive heat transfer properties.

In recent years, research on natural convection in U-shaped cavities filled with nanofluids has attracted considerable attention due to its potential applications in heat exchangers, cooling systems, and energy-efficient designs. Yuan et al. [1] conducted a simulation study to investigate the natural convection of nanofluids in a U-shaped cavity with a heating obstacle, examining the effect of the cavity's

*Corresponding author: mainuddin633@duet.ac.bd (Main Uddin Ahammad)

**Received:** 17 February 2025; **Accepted:** 28 February 2025; **Published:** 18 March 2025

aspect ratio on the heat transfer performance. Their findings indicated that the aspect ratio significantly influences the flow and thermal characteristics within the cavity, affecting the overall heat transfer efficiency. Yuan et al. [2] extended this work by exploring the impact of magnetic fields on nanofluid natural convection within a baffled U-shaped enclosure, highlighting the role of magnetohydrodynamics (MHD) in enhancing thermal transport in such systems.

Further studies, such as those by Esfe et al. [3] focused on the use of nanofluids in porous media within U-shaped enclosures. These studies utilized a two-phase mixture method to model the complex interactions between the nanofluid and the porous structure, revealing that the presence of porous media significantly altered the heat transfer behavior, making it more efficient under certain conditions. Other studies, such as those by Zemani et al. [4] have also investigated specific nanofluids, such as CuO-water nanofluids, in U-shaped enclosures with different geometries, demonstrating that the inclusion of additional features like T-shaped baffles can further enhance natural convection and heat transfer.

These investigations, combined with earlier works like those by Snoussi et al. [5] Sheikholeslami et al. [6] and Gümgüm and Tezer-Sezgin [7] emphasize the diverse factors affecting natural convection heat transfer in nanofluid-filled cavities. Selvakumar and Dhinakaran [8] studied the flow and heat transfer of nanofluids around a circular cylinder, emphasizing the impact of uncertainties in the nanofluid's effective properties. Their research highlights the significance of considering these uncertainties for accurate heat transfer predictions, which is essential for the effective design of nanofluid-based thermal systems. Several studies have examined the behavior of nanofluids in specific configurations. A. Sohankar et all [9] conducted a numerical study on forced convection of $Al_2O_3$- $H_2O$ nanofluid in rotating micro channels with hydrophilic and hydrophobic surfaces, revealing how surface properties affect flow dynamics and heat transfer in microelectronics and biomedical applications. Similarly, Zafar H. Khan et al. [10] investigated natural convection in a triangular fin-shaped cavity with a partially heated base, finding that nanofluids improve heat transfer in passive cooling systems. Cornelia Revnic et al. [11] studied natural convection in a rectangular cavity, showing that changes in viscosity significantly impact flow and temperature distributions, highlighting the importance of accurate fluid modeling. Tarikul Islam et al. [12] explored heat generation and absorption effects in a wavy triangular cavity, stressing the need for better modeling in thermal energy storage and harvesting. Cho et al. [13] examined the impact of $Al_2O_3$-water nanofluid on natural convection in a U-shaped cavity, emphasizing its role in enhancing thermal conductivity and heat dissipation. Likewise, Triveni et al. [14] performed a numerical analysis of laminar natural convection in an arch-shaped enclosure containing $Al_2O_3$-water nanofluid, further validating the contribution of nanoparticles to improved convective heat transfer. The fundamental understanding of nanofluid behavior is rooted in classical research, including Maxwell's [15] study on effective thermal conductivity and Brinkman's [16] formulation of viscosity in concentrated suspensions.

From the above literature review it is followed that no research has carried out yet like the chosen configuration with specific boundary conditions. The main purpose of the current study is to analyze natural convective flow and heat transfer inside a U-shaped device containing solid strip with the optimization of heat transfer performance for $Al_2O_3$-water nanofluid.

## 2. Problem Formulation

Figure 1 displays a U-shaped device with the same height and width which is taken unity, is filled with $Al_2O_3$-water nanofluid. A thermally insulated horizontal solid strip, which is 0.1 units high and 0.6 units long, is settled at the lower mid position of the considered domain. The upper cold rib and the bottom wall is maintained at constant temperatures $T_c$ and $T_h$, respectively while the rest walls are assumed as adiabatic. All solid boundaries along with the internal strip are set as rigid no slip walls which indicate velocity components $u$ and $v$ are zero. The density variation of the nanofluid and other thermo-physical properties are followed by the Boussinesq approximation. Fluid and nanoparticle properties have been given in Table 1.

***Table 1.*** *Thermo-physical properties of water and alumina at 20 ℃.*

| Property | Water | Alumina ($Al_2O_3$) |
|---|---|---|
| $C_p(Jkg^{-1}K^{-1})$ | 4179 | 765 |
| $\rho(kgm^{-3})$ | 997.1 | 3970 |
| $k(Wm^{-1}K^{-1})$ | 0.613 | 40 |
| $\beta(K^{-1})$ | $21 \times 10^{-5}$ | $0.85 \times 10^{-5}$ |
| $\sigma(\mu S/m)$ | 0.05 | $1 \times 10^{-10}$ |

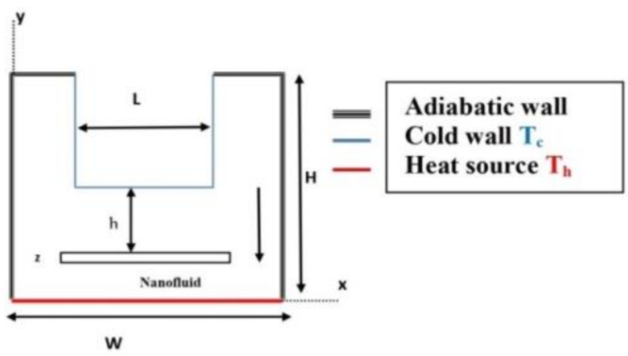


***Figure 1.*** *Geometry of the studied domain.*

The leading differential equations designed for the present problem described above in the dimensionless form consisting of the conservation of mass, momentum, and energy using nanofluid can be expressed as:

$$\frac{\partial U}{\partial X}+\frac{\partial V}{\partial Y}=0 \tag{1}$$

$$U\frac{\partial U}{\partial X}+V\frac{\partial U}{\partial Y}=-\frac{\partial P}{\partial X}+Pr\left(\frac{\rho_f}{\rho_{nf}}\right)\left(\frac{\mu_{nf}}{\mu_f}\right)\left(\frac{\partial^2 U}{\partial X^2}+\frac{\partial^2 U}{\partial Y^2}\right) \tag{2}$$

$$U\frac{\partial V}{\partial X}+V\frac{\partial V}{\partial Y}=-\frac{\partial P}{\partial Y}+Pr\left(\frac{\rho_f}{\rho_{nf}}\right)\left(\frac{\mu_{nf}}{\mu_f}\right)\left(\frac{\partial^2 V}{\partial X^2}+\frac{\partial^2 V}{\partial Y^2}\right)+\left(\frac{(\rho\beta)_{nf}}{\rho_{nf}\beta_f}\right)RaPr\theta \tag{3}$$

$$U\frac{\partial \theta}{\partial X}+V\frac{\partial \theta}{\partial Y}=\frac{\alpha_{nf}}{\alpha_f}\left(\frac{\partial^2 \theta}{\partial X^2}+\frac{\partial^2 \theta}{\partial Y^2}\right) \tag{4}$$

Where $Pr=\frac{\vartheta_f}{\alpha_f}$, $Ra=\frac{g\beta_f H^3(T_h-T_c)}{\vartheta_f\alpha_f}$, are the Prandtl number, and Rayleigh number respectively.

The equation (1) to (4) are made dimensionless by using the following relations

$$X=\frac{x}{H}, Y=\frac{y}{H}, U=\frac{uH}{\alpha_f}, V=\frac{vH}{\alpha_f}, \theta=\frac{T-T_c}{T_h-T_c}, P=\frac{pH^2}{\rho_{nf}\alpha_f^2} \tag{5}$$

Average Nusselt number at the heated wall of the enclosure is expressed as $Nu_{av}=\frac{-k_{nf}}{k_f}\int_0^1\frac{\partial\theta}{\partial X}dY$.

The boundary conditions for the problem is given below:

On the cold rib of the cavity: $U=V=0, \theta=0$

On the bottom wall of the cavity: $U=V=0, \theta=1$

On the remaining wall of the cavity and solid strip: $U=V=0, \frac{\partial\theta}{\partial N}=0$

The effective properties of nanofluid ($Al_2O_3$-water) are defined as follows:

***Table 2.*** *Applied model of some nanofluid properties.*

| **Nanofluid properties** | **Applied model** |
|---|---|
| Density | $\rho_{nf}=(1-\varphi)\rho_f+\varphi\rho_p$ |
| Specific heat | $(\rho C_p)_{nf}=(1-\varphi)(\rho C_p)_f+\varphi(\rho C_p)_p$ |
| Thermal diffusivity | $\alpha_{nf}=k_{nf}/(\rho C_p)_{nf}$ |
| Thermal expansion coefficient | $(\rho\beta)_{nf}=(1-\varphi)(\rho\beta)_f+\varphi(\rho\beta)_p$ |
| Dynamic viscosity based on Brinkman model [16] | $\mu_{nf}=\frac{\mu_f}{(1-\varphi)^{2.5}}$ |
| Thermal conductivity, according to the Maxwell model [15] | $k_{nf}=k_f\frac{(k_p+2k_f)-2\varphi(k_f-k_p)}{(k_p+2k_f)+\varphi(k_f-k_p)}$ |

## 3. Computational Procedure

The Galerkin weighted residual based finite element technique is applied for the studied problem to solve the governing equations numerically. In this method, at first the problem is defined as a two dimensional cavity and then the continuum domain is discretized into finite element meshes, which are composed of non-uniform triangular elements. Applying Galerkin method the governing partial differential equations are converted into a system of integral equations. Then boundary conditions are imposed and these nonlinear algebraic equations are modified into linear algebraic equations using Newton-Raphson iteration technique which are finally solved by triangular factorization method.

### 3.1. Grid Sensitivity Check

Different grid sizes of 2042, 3033, 4684, 11902, 30620, and 36784 elements are taken into consideration for the current simulation to test the independency of the results so that highest accuracy can be ensured. Average Nusselt number that represents the rate of heat transfer at the heated bottom surface are computed for these selected elements. Variations among the results for different number of elements are very minor that is followed from Table 3. Finally, based on the results from the table the grid consisting of 11902 elements are chosen for calculating average Nusselt number considering both the correctness of the numerical values and the corresponding solution time.

*Table 3.* *Average Nusselt number at hot bottom wall when Pr = 7, Ra = $10^4$, $\varphi$ = 0.05.*

| Number of elements | 2024 | 3033 | 4684 | 11902 | 30620 | 36784 |
|---|---|---|---|---|---|---|
| Nu | 1.0606 | 1.0603 | 1.0602 | 1.0599 | 1.0599 | 1.0598 |
| Deviation | | 0.0003 | 0.0001 | 0.0003 | 0.000 | 0.0001 |

### 3.2. Code Validation

For numerical code validation of the present problem, a computation is carried out to compare with the numerical study of CuO-water nanofuid natural convection in a U-shaped enclosure with a T-shaped baffle by Zemani *et al*. [4] shown in Figure 2. The comparison was carried out while employing the non-dimensional parameters: $Ra = 10^4, \Phi = 0.05, Pr = 7$. This figure shows that the streamline and isotherm patterns in the present work have excellent agreement with the reported studies by Zemani *et al*. [4]. These validations make an affirmation of the current numerical code.

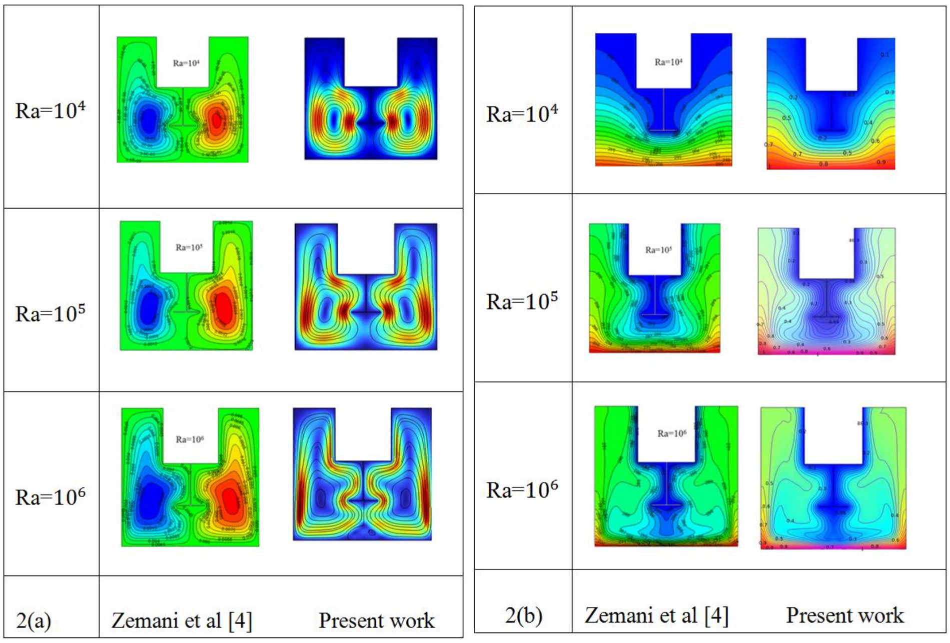


*Figure 2. Comparison of (a) streamlines and (b) isotherms between the work of Zemani et al. [4] and present for Cuo-water nanofliud at $\varphi$ = 0.05 and Pr = 7 varying Ra=$10^4 - 10^6$.*

## 4. Results and Discussions

To investigate the flow characteristics of nanofluids, various parameters were adjusted, including nanoparticle volume fractions ranging from, $\varphi$ = 0.01 to 0.1, Rayleigh numbers of Ra=$10^4$, Ra=$10^5$, Ra=$10^6$, Ra=$10^7$ a solid strip was placed at the center close to the bottom wall. Figure 3 clarify how the Rayleigh number affects the isotherms and streamlines. When the Rayleigh number is taken Ra=$10^4$, the streamlines appear relatively uniform, and minimal circulation indicates and the isotherm lines shift closer to the cold groove. In Rayleigh numbers of Ra=$10^5$ and Ra=$10^6$, convection controls heat transfer, creating stronger, well-defined vortices. The flow grows more dynamic, boosting thermal transport through dominant buoyancy-driven motion. And the isotherms exhibit significant variations: those isothermal lines increase aside the vertical wall. This behavior is due to increased buoyant forces associated with higher Rayleigh numbers. As the Rayleigh number grows, buoyant forces intensify, resulting in more vigorous fluid circulation. Consequently, heat transfer improves as the fluid more effectively transports heat from the hot surface to the cold surface. For the half of the cavity near the heat source indicating a large temperature. At lower Rayleigh numbers, such as Ra=$10^4$, conductive heat transfer lower at the higher Rayleigh numbers Ra=$10^7$, as Ra increases $10^4$ to $10^7$ convection becomes more dominant, resulting in stronger circulation patterns in the streamlines and more complex isothermal distributions. The use of $Al_2O_3$-water nanofluid enhances the heat transfer properties due to improved thermal conductivity, which affects both the temperature distribution and flow structure within the domain. The streamline patterns indicate the intensity and nature of convective currents, while the isothermal contours illustrate the heat distribution and temperature gradients. As a result, with a rise in the Rayleigh number, the efficiency of heat transfer is enhanced. These insights highlight the active interaction between conductive and convective heat transfer processes and the important function of buoyancy forces in affecting the thermal characteristics of nanofluids. Figure 3 displays two vortices: one rotating clockwise and the other counterclockwise on the both sides of the enclosure, respectively. These vortices are created due to the existence of the solid strip. In particular, the temperature variation between the heated fluid adjacent to the bottom wall and the external environment creates buoyancy forces that propel the fluid upward.

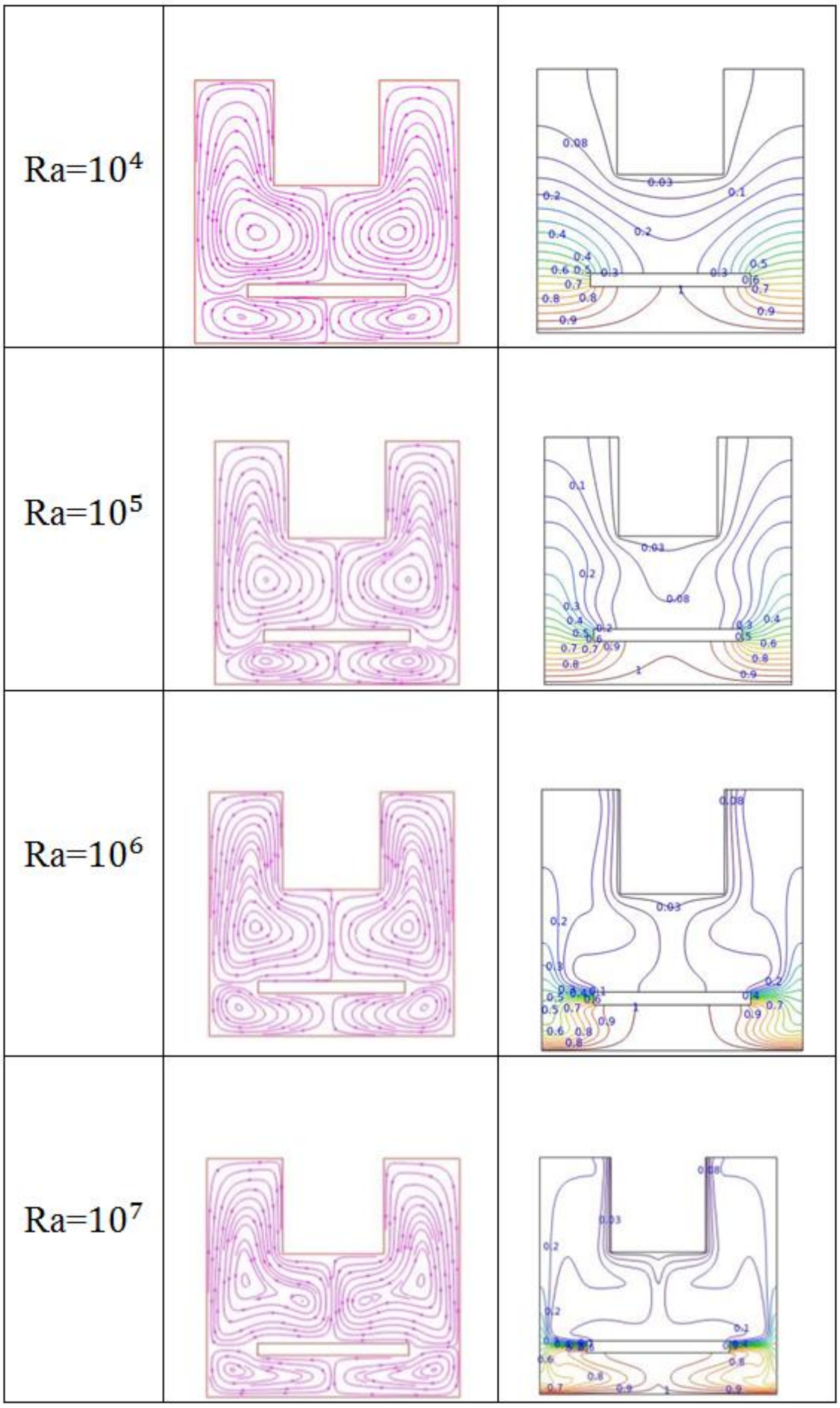


***Figure 3.*** *Streamlines and isotherms for different values of Rayleigh number Ra at $\varphi$ = 0.05 and Pr = 7.*

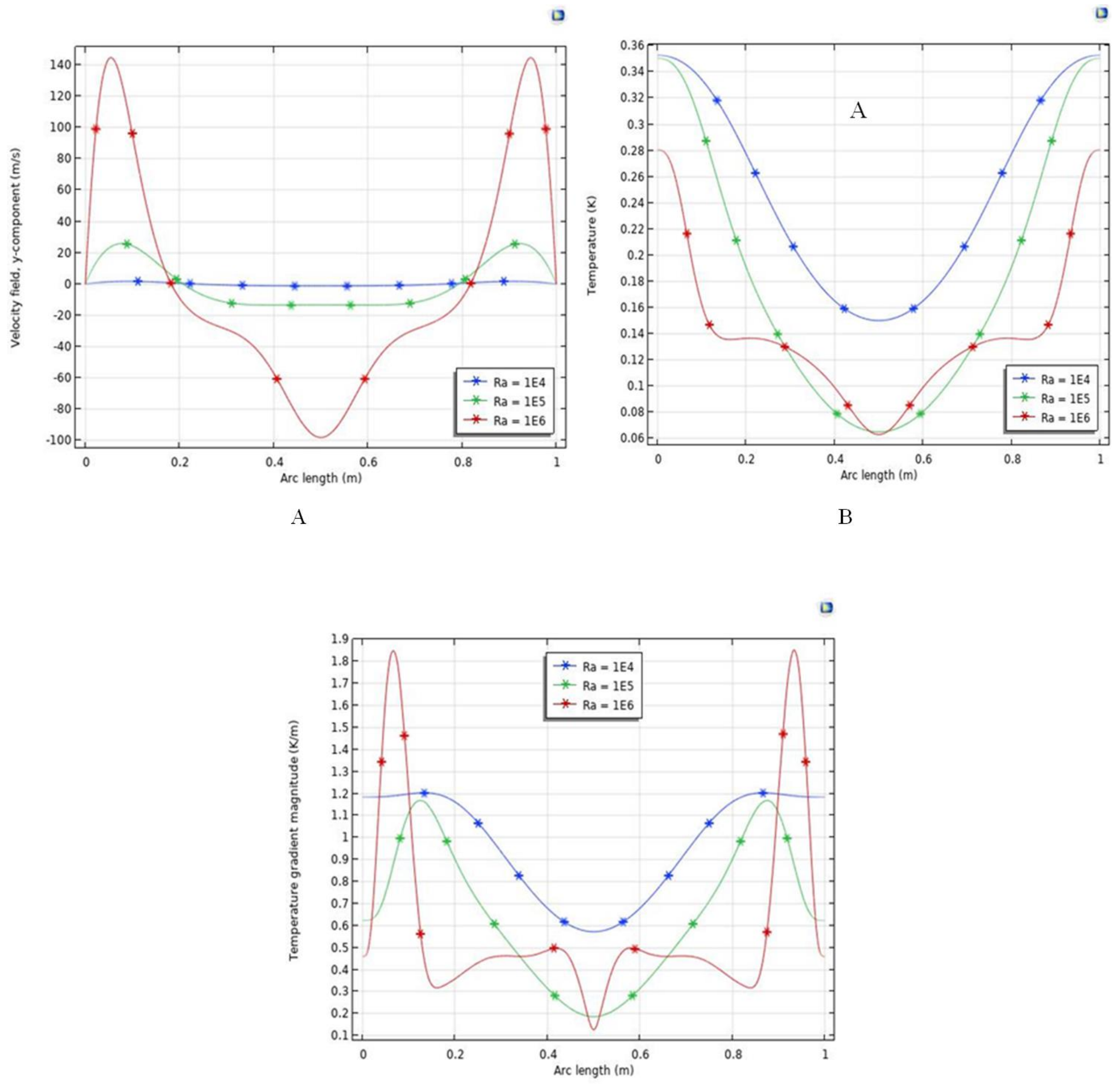


A B

C

***Figure 4.*** *(A) velocity profile, (B) temperature profile and (C) temperature gradient profile for the variation of Ra along the line y = 0.2.*

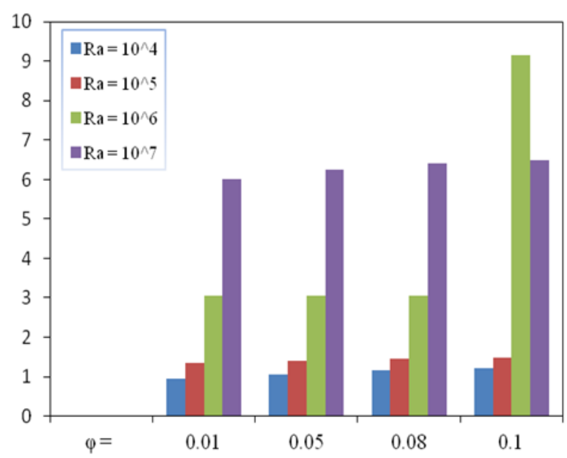


***Figure 5.*** *Average Nusselt number for variation of Ra versus volume fraction φ.s.*

Figure 4 (A) demonstrates the effect of $Ra = 10^4$, $Ra = 10^5$, $Ra = 10^6$ for the velocity profile. The range of velocity field y-component (m/s) is (-100 to 140) in the vertical line and the arc length is (0 to 1) on the horizontal line. The temperature profile is shown in the Figure 4 (B) which varies (0.06 to 0.36) in the vertical line for Ra variation. Particularly in case of 4 (C) where the variation of $Ra = 10^4$, $Ra = 10^5$, $Ra = 10^6$ is revealed for the temperature gradient magnitude (k/m) is (0.1 to 1.9) in vertical line and arc length (0 to 1) on the horizontal line.

Figure 5 presents the distribution of the average Nusselt number in the first column, second column, third and fourth column for volume fraction ($\varphi$ = 0.01- 0.1) and Rayleigh number ($Ra = 10^4$- $Ra = 10^7$). For various volume concentrations $\varphi$ = 0.01-0.1, relative to the average heat transfer of $Al_2O_3$ - pure water. Where $\varphi$ = 0.01 the average Nusselt Number for $Ra = 10^4$ touches 1 and $Ra = 10^5$ including 1 to 2, Ra=$10^6$ touches 3 and Ra=$10^7$ touches 6. Similarly $\varphi$ = 0.05-0.08 there are minor change Nu for Ra=$10^4$ to$10^7$. The last chart for $\varphi$ = 0.1 is the biggest change Nu for Ra=$10^6$.

Table 4 shows the relationship between the Rayleigh number (*Ra*) and the average Nusselt number ($Nu_{av}$). As *Ra* increases from $10^4$ to $10^7$, $Nu_{av}$ rises from 1.0599 to 6.2403, indicating a significant enhancement in convective heat transfer.

***Table 4.*** *Average Nusselt number at heated wall for different values of Ra when Pr=7 and =0.05.*

| Ra | $10^4$ | $10^5$ | $10^6$ | $10^7$ |
|---|---|---|---|---|
| $Nu_{av}$ | 1.0599 | 1.4024 | 3.0664 | 6.2403 |

To study the flow characteristics of nanofluids, different parameters were varied, including nanoparticle volume fractions ranging from $\varphi$ = 0.01 to 0.1. Furthermore, a solid body was positioned at the center of the heated slot on the bottom wall. Figure 6 illustrates the impact of the $\varphi$ on isotherms and streamlines. When $\varphi$ = 0.1, the streamlines reach their peak strength, they exhibit strong circulation and distinct vortex patterns and isotherm lines move closer to the cold groove. At $\varphi$ = 0.05 and $\varphi$ = 0.08, streamlines intensify, nanoparticles enhance thermal conductivity, improving heat transfer and circulation and the isotherms display noticeable changes. The isothermal lines shift and become more concentrated along the vertical wall, indicating enhanced thermal convection. This suggests an increased influence of buoyancy-driven flow, leading to greater heat transfer within the system. This phenomenon occurs due to the enhanced buoyant forces that accompany lower volume fraction. As it decreases, buoyant forces strengthen, leading to more active fluid circulation. As a result, heat transfer is enhanced, allowing the fluid to convey heat more efficiently from the hot surface to the cold surface. For $\varphi$ = 0.01, the streamlines are relatively weak, indicating a lower convective effect. The fluid motion remains sluggish and the isotherm lines become concentrated in the lower half of the cavity near the heat source, indicating a high-temperature region. At higher values, such as $\varphi$ = 0.1, conductive heat transfer is lower compared to lower value such as $\varphi$ = 0.01. As $\varphi$ decreases from $\varphi$ = 0.1 to $\varphi$ = 0.01, convection becomes more dominant, leading to stronger fluid circulation in the streamlines and more intricate isothermal patterns.

The streamlined patterns indicate the intensity and nature of convective currents, while the isothermal contours illustrate the heat distribution and temperature gradients. As a result, with the decrease in the $\varphi$, the efficiency of heat transfer is enhanced. These findings emphasize the dynamic interplay between conductive and convective heat transfer mechanisms, as well as the crucial role of buoyancy forces in shaping the thermal behavior of nanofluids. Figure 6 illustrates the presence of two distinct vortices one rotating clockwise and the other counterclockwise. These vortices emerge due to the influence of the solid strip structure within the system. Specifically, the temperature gradient between the heated fluid near the bottom wall and the surrounding environment generates buoyancy forces, driving the fluid upward and enhancing circulation. This process significantly impacts heat distribution, leading to more complex flow patterns within the cavity.

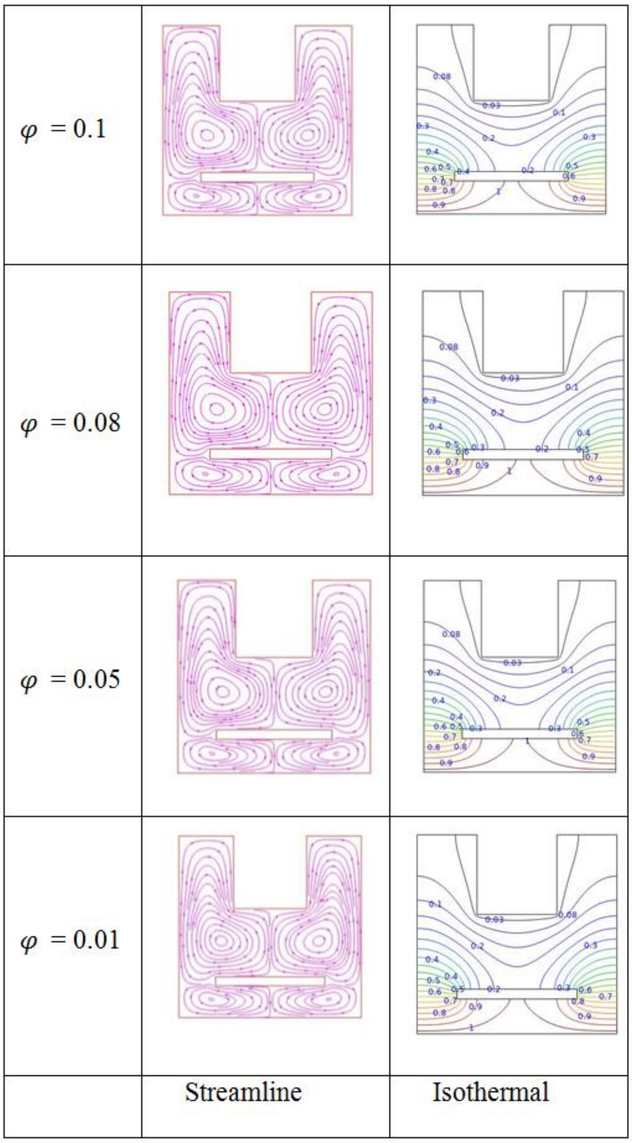


***Figure 6.*** *Streamlines and isotherms for different values of nanoparticle volume fraction $\varphi$ at Ra =$10^4$ and Pr = 7.*

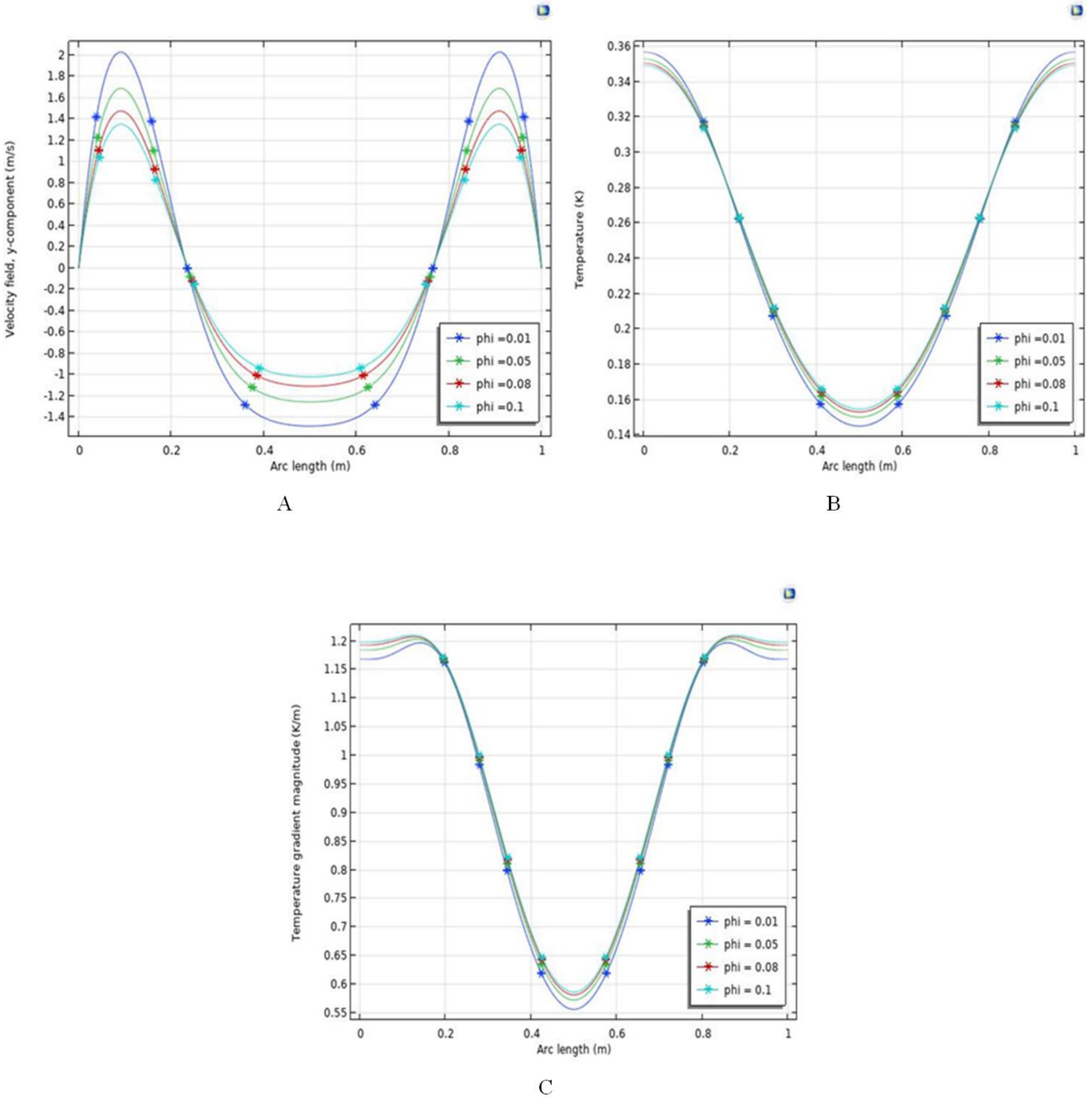


***Figure 7.*** *(A) velocity profile, (B) temperature profile and (C) temperature gradient profile for the variation of $\varphi$ along the line y = 0.2.*

Figure 7 (A) demonstrates the effect of $\varphi$ = 0.1, $\varphi$ = 0.05, $\varphi$ = 0.08 and $\varphi$ = 0.1. The range of velocity field y-component (m/s) is (-1.4 to 2) in the vertical line and the arc length is (0 to 1) on the horizontal line. In figure 7 (B) exposes the temperature (0.14 to 0.36) increases and decreases in the vertical line for $\varphi$ variation. Lastly, in case 7 (C) where clarify the variation of $\varphi$ = 0.1, $\varphi$ = 0.05, $\varphi$ = 0.08 and $\varphi$ = 0.1 numbers temperature gradient magnitude (k/m) is (0.55 to 1.2) in vertical line and arc length (0 to 1) on the horizontal line.

Figure 8 explores that the average Nusselt number in the first, second, third and fourth column of ($Ra$ =$10^4$- $Ra$ =$10^6$) and ($\varphi$ = 0.01- 0.1). For various natural convection $Ra = 10^4$ to$10^7$, relative to the average heat transfer of $Al_2O_3$ - water. Where $Ra$ =$10^4$-$10^5$ the average Nusselt Number for $\varphi$ = 0.01- 0.05 touches near 1 to 2, and $Ra$ =$10^6$ including 3 to 4 for $\varphi$ = 0.01- 0.08 and then only $\varphi$ = 0.1 changing highest Nusselt number $Ra$ =$10^6$ who's touches 9. The last chart for $Ra$ =$10^7$ is the major change Nu for Ra=$10^7$ in the previous $Ra$ Number.

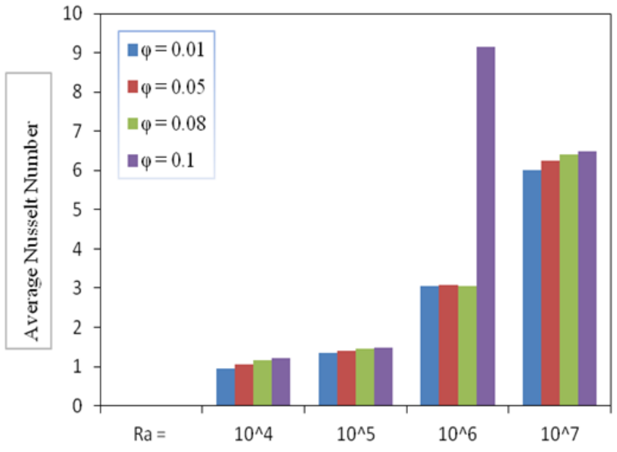


***Figure 8.*** *Average Nusselt number for variation of Ra versus volume fraction $\varphi$.*

*Table 5. Average Nusselt number at heated wall for different values of $\varphi$ when Pr=7 and Ra=$10^4$.*

| $\varphi$ | $0.01$ | $0.05$ | $0.08$ | $0.1$ |
|---|---|---|---|---|
| $Nu_{av}$ | 0.9514 | 1.0661 | 1.1592 | 1.2249 |

The correlation between volume fraction ($\varphi$) and the average Nusselt number ($Nu_{av}$) illustrates the impact of nanoparticle concentration on heat transfer efficiency which is shown in table 5. As $\varphi$ increases from 0.01 to 0.1, $Nu_{av}$ rises from 0.9514 to 1.2249, signifying an enhancement in convective heat transfer.

## 5. Conclusion

Natural convection in a U-shaped enclosure has been performed in the present work to observe the flow with the influence of thermal condition using $Al_2O_3$-water nanofluid. Temperature and velocity distribution are exposed graphically and in tabular form for visible understanding. In addition, average Nusselt number is computed varying with particle volume fraction and Rayleigh number. These may be summarized as below.

1. Fluid velocity and thermal field are affected much by the Rayleigh number than nanoparticle volume fraction.
2. Better heat transfer performance is recorded for larger values both of the parameters $Ra$ and $\varphi$.
3. Higher Rayleigh number plays a crucial role in heat transfer optimization.

## Abbreviations

| | |
|---|---|
| $C_p$ | Specific Heat (J kg$^{-1}$k$^{-1}$) |
| g | Gravitational Acceleration (ms$^{-2}$) |
| k | Thermal Conductivity (Wm$^{-1}$k$^{-1}$) |
| H | Cavity Side Height (m) |
| Nu | Average Nusselt Number |
| p | Dimensional Pressure (kgm$^{-1}$s$^{-2}$) |
| P | Non-dimensional Pressure ($(p + \rho gy)L^2/\rho u_i^2$) |
| Pr | Prandtl Number ($\vartheta/\alpha$) |
| Ra | Rayleigh Number ($g\beta\Delta T\,H^3/\nu\alpha$) |
| $T_h$ | High Temperature (K) |
| $T_c$ | Low Temperature (K) |
| (U, V) | Dimensionless Velocity Component |
| (x, y) | Dimensional Coordinates (m) |
| (X, Y) | Dimensionless Coordinates |
| α | Thermal Diffusivity (m$^2$s$^{-1}$) |
| β | Coefficient of Thermal Expansion (K$^{-1}$) |
| μ | Dynamic Viscosity (kg m$^{-1}$s$^{-1}$) |
| f | Fluid |
| nf | Nanofluid |
| p | Nanoparticle |

## Author Contributions

**Main Uddin Ahammad:** Conceptualization, Data curation, Formal Analysis, Software, Supervision, Writing – review & editing

**Shohag Hossain Reyad:** Conceptualization, Visualization, Writing – original draft

## Conflicts of Interest

The authors declare no conflicts of interest.

## References


[1] Ma Yuan, Rasul Mohebbi, M. M. Rashidi, Yang Zhigang. Simulation of nanofluid natural convection in a U-shaped cavity equipped by a heating obstacle: Effect of cavity's aspect ratio, Journal of the Taiwan Institute of Chemical Engineers. 2018, 93(5), 263-276. https://doi.org/10.1016/j.jtice.2018.07.026

[2] Yuan Ma, Rasul Mohebbi, M. M. Rashidi, Zhigang Yang, Mikhail A. Sheremet. Numerical study of MHD nanofluid natural convection in a baffled U-shaped enclosure, International Journal of Heat and Mass Transfer. 2019, 130, 123-134. https://doi.org/10.1016/j.ijheatmasstransfer.2018.10.072

[3] Mohammad Hemmat Esfe, Hossein Rostamian, Davood Toghraie, Maboud Hekmatifar, Amir Taghavi Khalil Abad. Numerical study of heat transfer of U-shaped enclosure containing nanofluids in a porous medium using a two-phase mixture method, Case Studies in Thermal Engineering. 2022, 38, Article-102150. https://doi.org/10.1016/j.csite.2022.102150

[4] Farah Zemani, Omar Ladjedel and Amina Sabeur Simulation of CuO-water nanofuid natural convection in a U-shaped enclosure with a T-shaped baffle, Journal of Engineering and Applied Science, 2023, 70: 99, https://doi.org/10.1186/s44147-023-00257-x

[5] Snoussi, Lotfi, Ouerfelli, Noureddine, Chesneau, Xavier, Chamkha, Ali J., Belgacem, Fethi Bin Muhammad, Guizani, Amenallah. Natural Convection Heat Transfer in a Nanofluid Filled U-Shaped Enclosures: Numerical Investigations. Heat Transfer Engineering, 2018, 39(16), 1450-1460. https://doi.org/10.1080/01457632.2017.1379343

[6] Mohsen Sheikholeslami, Mofid Gorji-Bandpy, Kuppalapalle Vajravelu. Lattice Boltzmann simulation of magnetohydrodynamic natural convection heat transfer of $Al_2O_3$ water nanofluid in a horizontal cylindrical enclosure with an inner triangular cylinder". International Journal of Heat and Mass Transfer. 2015, 8, 15-26. https://doi.org/10.1016/j.ijheatmasstransfer.2014.08.090

[7] S. Gümgüm, and M. Tezer-Sezgin. DRBEM Solution of Mixed Convection Flow of Nanofluids in Enclosures with Moving Walls, Journal of Computational and Applied Mathematics, 2014, 259, 730–740. https://doi.org/10.1016/j.cam.2013.05.006

[8] Deepak Selvakumar R, Shanmugam Dhinakaran. Nanofluid flow and heat transfer around a circular cylinder: A study on effects of uncertainties in effective properties. Journal of Molecular Liquids, 2016, 223, Article-572. https://www.researchgate.net/publication/328401868

[9] A. Sohankar, M. Riahi, E. Shirani. Numerical Study of Water/$Al_2O_3$ Nanofluid Forced Convection in a Rotating Hydrophilic and Hydrophobic Microchannel. Journal of Applied Fluid Mechanics, 2019, 12(1), 212-231. https://www.jafmonline.net/article_735.html

[10] Zafar H. Khan, Waqar A. Khan, Ahmed M. R. Elbaz, Muhammad Qasim, Sayer O. Alharbi, Licheng Sun. Natural convection in triangular fin-shaped cavity with partially heated base using nanofluid. Journal of Applied Mathematics and Mechanics. 2021, 101(12), https://doi.org/10.1002/zamm.202000306

[11] Cornelia Revnic, Eiyad Abu-Nada, Teodor Grosan, Ioan Pop. Natural convection in a rectangular cavity filled with nanofluids: Effect of variable viscosity. International Journal of Numerical Methods for Heat & Fluid Flow. 2018, 28(6), 1410-1432. https://doi.org/10.1108/HFF-06-2017-0244

[12] Tarikul Islam, Md. Nur Alam, Shafiullah Niazai, Ilyas Khan, Md. Fayz-Al-Asad & Sultan Alqahtani. Heat generation/absorption effect on natural convective heat transfer in a wavy triangular cavity filled with nanofluid. Journal of Scientific Reports. Scientific Reports, 2023, 13(1), Article-21171. https://doi.org/10.1038/s41598-023-48704-2

[13] Cho Ching-Chang, Yau Her-Terng, Chen Cha'o-Kuang,. Enhancement of natural convection heat transfer in a U-shaped cavity filled with $Al_2O_3$-water nanofluid. Thermal Science, 2012, 16(5), 1317-1323, https://doi.org/10.2298/TSCI1205317C

[14] M. K. Triveni, D. Sen and R. Panua. Numerical Study of Laminar Natural Convection in an Arch Enclosure Filled with $Al_2O_3$-Water Based Nanofluid. Journal of Applied Fluid Mechanics. July 2016, 9(4), 1927-1936 https://doi.org/10.18869/acadpub.jafm.68.235.24798

[15] Maxwell JC (1904) A treatise on electricity and magnetism, 2nd edn. Oxford University Press, Cambridge, pp 435–441 46.

[16] Brinkman HC (1952) the viscosity of concentrated suspensions and solutions. J Chem Phys 20: 571–58.